bjh research paper

Diagnostic value of whole-body ultra-low dose computed tomography in comparison with spinal magnetic resonance imaging in the assessment of disease in multiple myeloma

Davide Ippolito,[1,2] Cammillo Talei Franzesi,[1,2] Sara Spiga,[1,2] Valeria Besostri,[1,2] Sara Pezzati,[3] Fausto Rossini[3] and Sandro Sironi[2,4]

[1]Department of Diagnostic Radiology, San Gerardo Hospital, [2]School of Medicine, University of Milano-Bicocca, [3]Department of Haematology, San Gerardo Hospital, Monza, MB, and [4]Department of Diagnostic Radiology, Papa Giovanni XXIII Hospital, Bergamo, Italy

Received 17 October 2016; accepted for publication 23 November 2016

Correspondence: Davide Ippolito, Department of Diagnostic Radiology, University of Milano-Bicocca, H S.Gerardo, Via Pergolesi 11, 20900 – Monza, Milan, Italy.
E-mail: davide.atena@tiscalinet.it

Summary

This study compared the diagnostic value of Whole-Body Ultra Low-Dose computed tomography (WBULDCT) with that of Spinal Magnetic Resonance Imaging (SMRI) in identification of spinal bone marrow involvement in patients with Multiple Myeloma (MM). Thirty-five patients with histologically proven MM underwent WBULDCT and dedicated SMRI. Unenhanced WBULDCT was performed on a 256-slice scanner, with 120 kV and 40 mAs. SMRI was performed on a 1·5T magnet, with T1-turbo spin echo and T2-short tau inversion recovery sequences on sagittal plane. WBULDCT was compared with SMRI in terms of lesion detection, pattern and bone marrow involvement. The overall concordance between WBULDCT and SMRI in lesion detection was 76·7%, detecting (25/35) or excluding (8/35) involvement of the axial skeleton, while in 2/35 patients WBULDCT and SMRI were discordant in terms of axial skeleton involvement. The concordance in spinal distribution of lesions was 61·6% on cervical, 71·5% on dorsal, 86·4% on lumbar and 94·4% on sacral, while for the pattern of disease, it was 56·1% for the focal and 88·7% for the combined pattern. Cohen's kappa index was 0·85 ($P < 0·001$) assessing an excellent agreement. WBULDCT represents a useful diagnostic tool in the detection of spinal involvement of MM patients, offering detailed information about extra-axial involvement, which could be potentially missed with dedicated SMRI.

Keywords: whole-body ultra-low dose CT, spinal magnetic resonance imaging, mutlitple myeloma, low-grade non-Hodgkin B-cell lymphoma, lytic bone lesions.

Multiple myeloma (MM) represents the second most common haematological malignancies (10–15% of all) and 1% of all malignant diseases; it is characterized by a clonal proliferation of antibody-secreting plasma cells in the bone marrow microenvironment. The proliferating plasma cells infiltrate the bone marrow, leading to replacement of the normal myelopoiesis, bone destruction and marrow failure (Ippolito *et al*, 2013; Sachpekidis *et al*, 2015; Song *et al*, 2015).

The detection of lytic bone lesions represents a criterion defining a symptomatic MM that requires treatment, even in the absence of clinical symptoms (Lecouvet *et al*, 2001; Mahnken *et al*, 2002; Derlin & Bannas, 2014). The axial skeleton is the most common site of myelomatous lesions, arising in 90% of patients during the course of their disease, with a various spectrum of presentation, such as myeloma-induced osteoporosis, osteolysis or compression fractures and, in almost 20% of the cases, spinal cord compression may occur (Bird *et al*, 2011; Wight *et al*, 2015).

The typical imaging findings on conventional radiography and computed tomography (CT) include punched out lytic bone lesions, diffuse osteopenia, fractures and, rarely, osteosclerosis. In particular, diffuse heterogeneous osteopenia may be difficult to differentiate from perimenopausal and senile osteoporosis (Mahnken *et al*, 2002; Baur-Melnyk *et al*, 2008).

Magnetic resonance imaging (MRI) has the ability to distinguish between physiological or pathological bone marrow

First published online 24 February 2017
doi: 10.1111/bjh.14545

osteoporosis involvement, and is currently the standard of care in this setting (Zamagni *et al*, 2011).

Multiple myeloma staging has traditionally relied on serum and urine markers of disease as well as conventional radiography. The first widely accepted staging system, the Durie and Salmon system, was reported in 1975 and is based on levels of haemoglobin, serum calcium, and M protein and on the extent of bone involvement depicted on radiographs (Durie & Salmon, 1975).

The detection of skeletal myelomatous involvement is critical in the staging, treatment planning and assessment of prognosis in MM; for these reasons and considering the importance of the assessment of tumour burden, more sophisticated cross-sectional imaging techniques are being established for the diagnosis of MM (Lecouvet *et al*, 1999; Hanrahan *et al*, 2010).

In 2003, the Durie and Salmon staging system was adapted to incorporate cross-sectional imaging information. This modified Durie and Salmon staging system (called the "Durie and Salmon Plus" system) allows better detection of early disease and a more precise differentiation between patients with stage II disease from those with stage III disease (Durie *et al*, 2003).

More recently, practical guidelines from the European Society for Medical Oncology (ESMO) (Moreau *et al*, 2013) and the International Myeloma Working Group (IMWG) updated criteria for the diagnosis of MM (Rajkumar *et al*, 2014) have been defined for MM diagnosis, which recommend the use of both MRI and CT, with specific indications and with a particular focus on spinal involvement.

In particular, MRI is needed in when a skeletal survey is negative or ambiguous (such as equivocal lytic lesions, especially in parts of the skeleton which are difficult to visualize on plain radiographs, such as ribs, sternum and scapulae), the patient is symptomatic and bone involvement is suspected. Moreover, a dedicated spinal MRI evaluation is necessary in case of suspected spinal cord compression (Dimopoulos *et al*, 2011; Moreau *et al*, 2013; Rajkumar *et al*, 2014).

Multidetector CT (MDCT) has been demonstrated in several studies to have an improved sensitivity over that of the radiographic skeletal survey for evaluation of the extent of lytic bone involvement, allowing the detection of smaller lesions and of extra-osseous manifestations of MM, and the acquired 3D data sets can be used for radiation therapy planning if needed.

Positron emission tomography (PET)/CT is a useful tool for prognostic and predicting therapy response, because it offers reliable data regarding the complete response and stringent complete response categories as well as for disease progression (Spinnato *et al*, 2012; Derlin *et al*, 2013), according to the faster changes in imaging findings that occur in patients who respond to therapy (Terpos *et al*, 2015).

MDCT also allows the assessment of fracture risk and characterization of compression fractures (Regelink *et al*, 2013; Pianko *et al*, 2014; Martí-Bonmatí *et al*, 2015). However, CT has limited sensitivity for detection of diffuse bone marrow infiltration, bone marrow lesions without lytic reaction (Derlin & Bannas, 2014).

Given that the most recent guidelines for the management of MM-related complications (Terpos *et al*, 2015) identified whole-body ultra-low dose CT (WBLDCT) as being more sensitive than conventional radiography for depicting osteolytic disease, it was recommended as the novel standard technique for the detection of lytic lesions in myeloma (Terpos *et al*, 2015).

Conversely, MRI currently represents the elective imaging technique for assessing the degree of bone marrow plasma cell infiltration, due to its ability to study large volumes of bone marrow without radiation exposure, and its higher contrast resolution and discrimination power. It is considered the gold standard technique for the assessment of myelomatous involvement of the spine, due to its better sensitivity, allowing the identification of spinal cord and/or nerve root compression, and the recognition of soft tissue masses (Dimopoulos *et al*, 2009; Zamagni & Cavo, 2012; Martí-Bonmatí *et al*, 2015).

MRI can also predict the risk of vertebral fracture and is the best diagnostic tool for differentiating between physiological and myeloma-infiltrated bone marrow and between benign and malignant vertebral fractures (Hanrahan *et al*, 2010; Zamagni & Cavo, 2012).

Hence, the purpose of our study was to compare the diagnostic value of WBULDCT with Spinal MRI (SMRI) in the identification of spinal bone marrow involvement in patients with MM.

Materials and methods

Study population

We retrospectively evaluated a total of 35 patients (21 males; 14 females; age range 52–83 years), with histologically proven MM, who underwent WBULDCT and dedicated SMRI, 9/35 for staging purpose and 26/35 during the follow-up of the disease.

WBULDCT protocol

Unenhanced WBULDCT studies were obtained on a 256-slice scanner (iCT, Philips, Eindhoven, the Netherlands), with the following protocol: tube voltage 120 kV, tube current time product 40 mAs, collimation 128 × 0·65. Patients were positioned supine and head first, with the arms beside the body to allow evaluation of the upper limbs. The Field of View (FOV) was adapted to the largest circumference of the patient. The scan length was stretched from the roof of the skull down to the proximal tibial metaphysis. The images were acquired in inspiratory apnoea during the scanning through the thorax and the upper abdomen. Depending on

Table I. Whole-body ultra-low-dose computed tomography (WBULDCT) study protocol.

WBULDCT
Scanner: 256-row (iCT, Philips)
Scan length: from the vertex down to the knees
Tube voltage/current: 120 kV/40 mAs
Collimation: 128 × 0·65
Thickness: 2 mm
Effective radiation dose: 4·2 mSv
Acquisition time: 10 s

patients' height, the scan lasted about 10 s (range, 8·7–12·5 s). As the intrinsic bone contrast was high, we were able to reduce the tube current to 40 mAs, resulting in a mean effective equivalent dose delivered to the patient of 4·2 mSv (Table I).

SMRI protocol

SMRI examinations were performed on a 1·5 T magnet (Achieva, Philips). The patient was positioned head first (supine), using the spine coil to evaluate the whole axial skeleton. All SMRI studies were performed in stepping-table movement.

T1-weighted turbo spin echo (TSE; echo time [TE] 10 ms; repetition time [TR] 400 ms; FOV 400; thickness 4 mm) and T2-weighted Short Tau inversion recovery (STIR; TE 10 ms; TR 2000 ms; FOV 400; thickness 4 mm) sequences were performed on the sagittal plane.

The mean acquisition time was approximately 15 min (Table II).

Image analysis

All WBULDCT and SMRI images were independently assessed by one (blinded) radiologist with 10 years experience.

Images were evaluated according to the different patterns of bone marrow involvement: normal appearing bone marrow (dependent upon fatty:haemopoietic cells ratio), focal myeloma lesions, diffuse bone marrow infiltration and combined.

On WBLDCT, the diagnosis of osteolytic bone lesions was performed on the basis of axial and multiplanar reformatted (MPR) images, whereas the assessment of spinal involvement in terms of infiltration patterns was assessed using MPR images on sagittal and coronal planes. Only typical, punched-out osteolyitic areas that showed no sclerotic rim or cystic content were recorded as focal myeloma involvement. We considered the presence of a diffuse reduction of bone mineral density on CT scan was considered to be a diffuse pattern and a combined pattern was recorded when the presence of both focal lesions and diffuse infiltration was seen.

On SMRI, the diagnosis of bone marrow involvement was performed using T1-weighted TSE and fat-suppressed sequences (STIR), which are sensitive for the detection of bone marrow alterations. Pathological replacement (circumscribed/focal or homogeneous diffuse) of bone marrow leads to a modification of the signal intensity, causing a decrease in the signal intensity on T1-weighted TSE and an increase in the signal intensity on T2-weighted STIR images; these alterations were recorded as myeloma involvement. In particular, focal myeloma involvement was considered to be an accumulation of myeloma cells when a focal area of low signal intensity on T1-weighted spin-echo images was found in the bone marrow corresponding to high signal intensity on STIR images.

Diffuse infiltration was diagnosed when the bone marrow was diffusely reduced in signal on T1-weighted spin-echo images and increased on STIR images.

Table II. SMRI study protocol.

SMRI		
1·5 T magnet (Achieva, Philips), Spine coil		
Scan length: whole axial skeleton on the sagittal plane		
T1 TSE	TE 7·2 ms (6–18)	TR 400 ms (200–600)
T2 STIR	TE 80 ms (60–150)	TR 2000 ms (>1800)
DFOV: 400		
Thickness: 4 mm		
Acquisition time: 15 min		

DFOV, display field of view; SMRI, spinal magnetic resonance imaging; STIR, short tau inversion recovery; TE, echo time; TR, repetition time.

Statistical analysis

Cohen's kappa was used to summarize the agreement between WBULDCT and SMRI. The 95% confidence intervals for the Cohen's kappa index were also reported.

A $P < 0{\cdot}05$ was considered as statistically significant (Table III).

Results

Our series included a total of 35 MM patients in whom the myelomatous spinal involvement was analysed using

Table III. Interpretation guidance for strength of agreement on Cohen's kappa index.

Kappa coefficient	Strength of agreement
<0·00	Poor
0·00–0·20	Slight
0·21–0·40	Fair
0·41–0·60	Moderate
0·61–0·80	Substantial
0·81–1·00	Almost perfect

Table IV. Total number of identified focal myelomatous lesions within the axial skeleton on WBULDCT and SMRI according to pattern of bone marrow involvement.

Pattern of bone marrow involvement		SMRI	WBULDCT
Focal	11/35 (31·42%)	55	98
Diffuse	5/35 (14·28%)	0	0
Combined	11/35 (31·42%)	149	168
Negative	8/35 (21·85%)	0	0
Total		204	266

SMRI, spinal magnetic resonance imaging; WBULDCT, whole-body ultra-low-dose computed tomography.

WBULDCT and SMRI imaging. The bone marrow involvement was classified into 4 different patterns: focal, diffuse, combined and negative. The infiltration patterns were concordant in both techniques, finding 11 focal pattern (31·42%), 5 diffuse pattern (14·28%), 11 combined pattern (31·42%) and 8 negative pattern (21·85%) (Table IV).

We found a total of 687 lesions on WBULDCT (subdivided on 266 axial lesions and 421 extra-axial lesions) and 204 axial lesions on SMRI. Analyzing the spinal anatomic distribution of myelomatous lesions within the focal and combined pattern of disease, WBULDCT identified 73 lesions (27·44%) that were localized on the cervical spine, 137 (51·5%) on the dorsal spine, 38 (14·28%) on the lumbar spine and 18 (6·76%) on the sacral spine, while SMRI detected 45 lesions (22·05%) that were localized on the cervical spine, 98 (48·03%) on the dorsal spine, 44 (21·56%) on the lumbar spine and 17 (8·33%) on the sacral spine (Table V).

The overall concordance between WBULDCT and SMRI in the detection of myelomatous lesions within the axial skeleton was 76·7%. In particular, both techniques showed no evidence of myelomatous lesions in 8/35 (22·85%) patients, and they were both positive in 25/35 (71·42%).

WBULDCT and SMRI were discordant in only 2 (5·71%) patients: 1 patient was positive on WBULDCT and negative on SMRI and 1 patient was negative on WBULDCT and positive on SMRI (Table VI).

The concordance in the spinal anatomic distribution of myelomatous lesions was 61·6% on the cervical spine, 71·5% on the dorsal spine, 86·4% on the lumbar spine and 94·4% on the sacral spine, while the concordance according to the pattern of disease was 56·1% for the focal pattern and 88·7% for the combined pattern. The Cohen's kappa index was 0·85 ($P < 0·001$) assessing an excellent agreement.

Table V. Spinal anatomic distribution of myelomatous lesions within the focal and combined patterns of disease.

Spinal anatomic distribution of myelomatous lesions	SMRI	WBULDCT
Cervical	45 (22·05%)	73 (27·44%)
Dorsal	98 (48·03%)	137 (51·50%)
Lumbar	44 (21·56%)	38 (14·28%)
Sacral	17 (8·33%)	18 (6·76%)
Total	204	266

SMRI, spinal magnetic resonance imaging; WBULDCT, whole-body ultra-low-dose computed tomography.

In terms of Durie and Salmon Staging System Plus agreement, WBULDCT and SMRI were concordant in 29/35 (82·85%) patients: specifically 20 patients were stage I, 7 patients were stage II and 2 patients were stage III. The Cohen's kappa index was 0·66 ($P < 0·05$) assessing a substantial agreement.

When classifying patients according to disease stage, WBULDCT and SMRI were discordant in 6/35 (17·14%) patients: 1 patient was considered stage I on WBULDCT and stage II on SMRI, 1 patient was stage II on WBULDCT and stage I on SMRI, 2 patients were stage III on WBULDCT and stage I on SMRI and 2 patients were stage III on WBULDCT and stage II on SMRI (Table VII).

Discussion

Radiology plays an important role in staging, monitoring treatment response, assessing complications and detecting disease recurrence in MM patients.

Almost 80% of MM patients will have radiological evidence of skeletal involvement and the axial skeleton is the most common site of myelomatous lesions, arising in almost 90% of patients, with a various spectrum of presentation, such as myeloma-induced osteoporosis, osteolysis or compression fractures, often having a large impact on the patient's quality of life (Hanrahan *et al*, 2010; Pianko *et al*, 2014).

Therefore, considering the importance of the assessment of tumour burden, an accurate diagnosis and staging are necessary.

Conventional radiology has been an integral part of the staging system in MM for the last 35 years; unfortunately, its sensitivity for osteolytic lesions detection is very low, as they

Table VI. Concordance between WBULDCT and SMRI in the evaluation of axial skeletal involvement.

	WBULDCT		
SMRI	*0*	*1*	Total
0	8	1	9 (25.7%)
1	1	25	26 (74.3%)
Total	9 (25.70%)	26 (74.30%)	35
Weighted Kappa[a]	0.85		
Standard error	0.102		
95% CI	0.65–1.0		
Linear weights			

95% CI, 95% confidence interval; SMRI, spinal magnetic resonance imaging; WBULDCT, whole-body ultra-low-dose computed tomography.

Table VII. Classification within WBULDCT and SMRI according to Durie and Salmon staging system PLUS depending on the number of lesions or the grade of diffuse disease.

	WBULDCT			
SMRI	Stage I	Stage II	Stage III	Total
Stage I	20	1	2	23 (65·7%)
Stage II	1	7	2	10 (28·6%)
Stage III	0	0	2	2 (5·7%)
Total	21 (60·00%)	8 (22·90%)	6 (17·10%)	35
Weighted kappa[a]	0·663			
Standard error	0·12			
95% CI	0·427–0·899			
Linear weights				

Stage I: <5 lesions or mild diffuse disease; Stage II: 5 – 20 lesions or moderate diffuse disease; Stage III: >20 lesions or severe diffuse disease.
95% CI, 95% confidence interval; SMRI, spinal magnetic resonance imaging; WBULDCT, whole-body ultra-low-dose computed tomography.

can be only detected when more than 30% of trabecular loss is evident. Finally, plain radiographs may show non-specific abnormalities that require further characterisation by other techniques (Lecouvet *et al*, 1999; Durie *et al*, 2003).

Therefore, according to the most recent literature, we have incorporated more sophisticated cross-sectional imaging techniques in the diagnostic workout of MM. In particular, as confirmed by several studies, such as those by Rajkumar *et al* (2014) and Martí-Bonmatí *et al* (2015), MRI and CT have been shown to be more sensitive than radiographic skeletal survey in the detection of myeloma infiltration (Ghanem *et al*, 2006; Rajkumar *et al*, 2014).

For these reasons WBLDCT is currently recommend as the novel standard procedure for the diagnosis of lytic disease in patients with MM grade 1A (Rajkumar *et al*, 2014).

The routine use of PET imaging may be useful in selected cases for clarification of previous imaging findings, preferably within a trial, and in the evaluation of therapy response (Terpos *et al*, 2015). It might also be a useful technique for determining survival and prognosis, even if the high radiation dose exposure, cost and reduced availability may represent issues in clinical practice (Bird *et al*, 2011).

WBULDCT was introduced by Horger *et al* (2007, 2008) as a preferable alternative to conventional radiology in clinical practice, demonstrating that even the low-dose protocol is appropriate for the diagnosis of lytic lesions and suggesting that WBULDCT may be used not only for the diagnosis of lytic bone lesions in MM but also for the direct visualization of bone marrow and extramedullary myeloma involvement.

The efficacy of low-dose CT protocols has been assessed in several studies, dealing with extra-osseous findings or the involvement of other organs. Also, multiplanar reconstructions (MPR) increase CT accuracy, allowing the problem of the overlapping of soft tissues and bony structures to be overcome (Gleeson *et al*, 2009; Ippolito *et al*, 2013).

WBULDCT should be primarily considered in symptomatic patients with bone pain and lack of evidence of osteolytic lesions on the skeletal survey and/or in patients for whom MRI is contraindicated (claustrophobia or metal devices in the body) (Bird *et al*, 2011).

However, MM may present with osteopenia alone in almost 10% of patients and could be potentially confused with postmenopausal or senile osteoporosis, if monoclonal gammopathy and marrow plasmacytosis are not detected (Weinstein, 1992; Collins, 2004).

Unfortunately, one of the main limitations of WBULDCT is its low specificity for the evaluation of diffuse bone marrow infiltration (e.g. osteopenia pattern). The best evaluation of diffuse pattern is actually performed using MRI, which offers a direct, high-contrast and sensitive assessment of bone marrow composition and distribution (Lecouvet *et al*, 1999; Shortt *et al*, 2009).

Moreover, CT is has a reduced ability to differentiate between insufficiency and pathological fractures, while MRI allows the assessment of the infiltration of the bone marrow by neoplastic cells and the displacement of fat cells too, representing the best diagnostic tool, especially in those symptomatic patients who have negative or ambiguous findings on WBULDCT (Figs 1 and 2).

In fact, since the report by Moulopoulos *et al* (1995), several, more recent, studies as reviewed by Martí-Bonmatí *et al* (2015), have assessed the role of MRI in the characterization of bone marrow cellularity and its ability to distinguish vertebral collapse due to disease from that due to accompanying osteoporosis (Gleeson *et al*, 2009).

In particular, in insufficiency fractures, fat signal is preserved on T1-weighted images, a retropulsed bone fragment is present and horizontal band-like areas representing the fracture plane and fluid collection are seen. In pathological fractures, the posterior cortex is convex toward the spinal canal (Fig 1), an epidural or paravertebral mass is visible and the entire vertebral body or pedicles have low signal on T1 weighted images. Normal marrow fat in benign fractures results in suppression of the signal intensity on STIR images (Fig 1) whereas, in pathological fractures, the tumour lacks

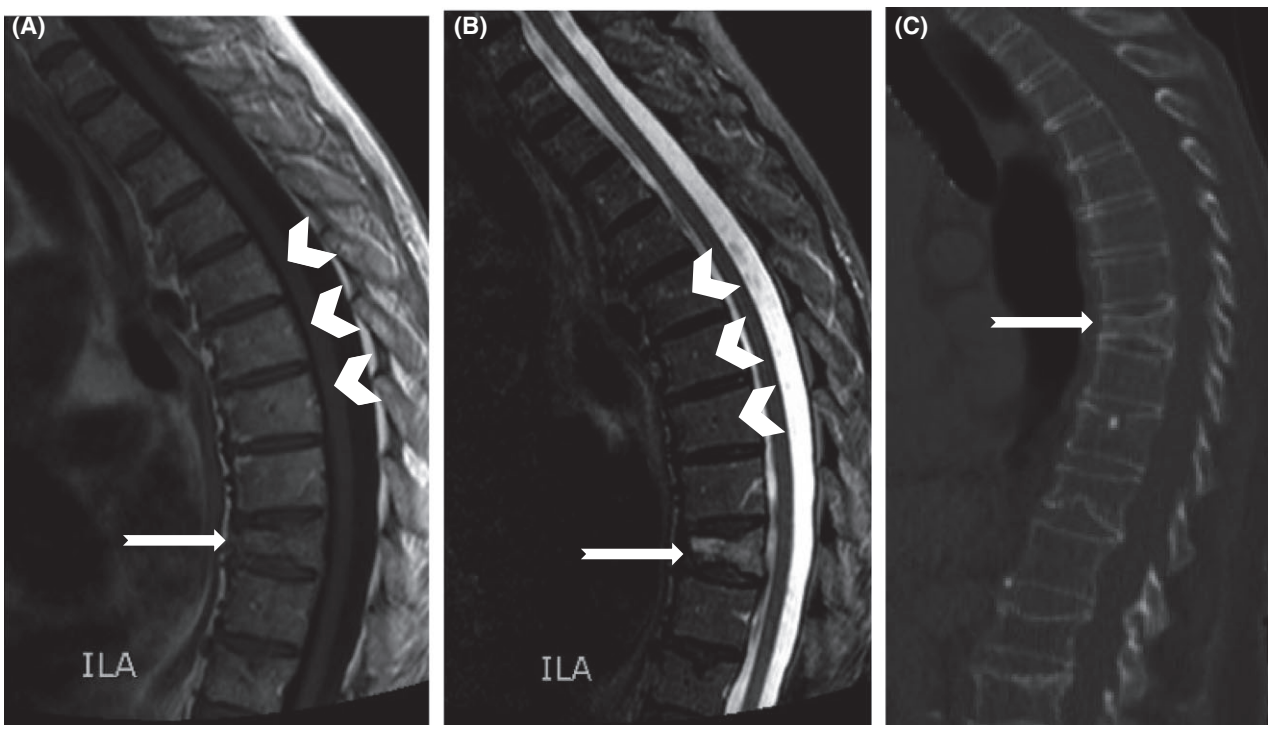

Fig 1. Patient aged 56 years with focal pattern, evaluated during the staging of the disease. Sagittal T1-weighted (A) short tau inversion recovery (STIR) (B) and computed tomography scan images (C) of the dorsal spine show an insufficiency fracture of a dorsal vertebral body (arrows). Normal signal intensity is shown in other vertebral bodies in T1 weighted (A) and STIR weighted (B) images (arrowheads) and slightly higher signal intensity in the STIR image (arrow) due to the bone marrow oedema.

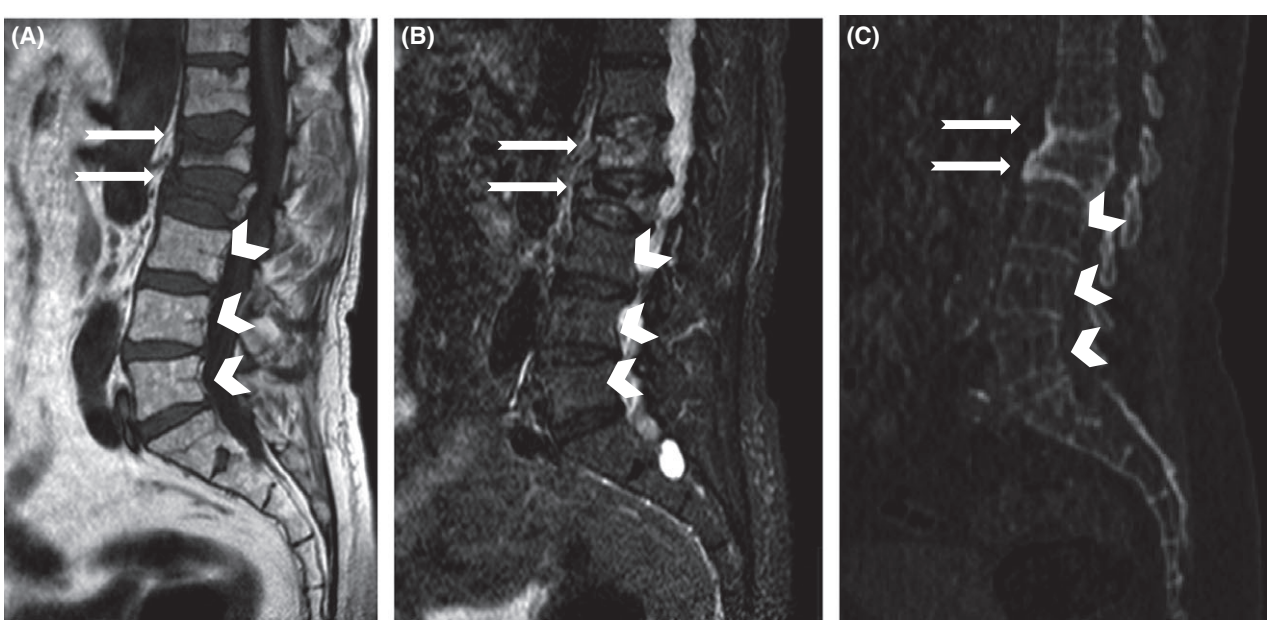

Fig 2. Patient aged 78 years with focal pattern, evaluated during the staging of the disease. Sagittal T1-weighted (A), short tau inversion recovery (STIR) (B) and computed tomography (CT) scan images (**C**) of the lumbar spine show a focus of plasma cell infiltration and a pathological fracture in the L1 and L2 vertebras (arrows) with low signal intensity in the T1 weighted image (A), and high signal intensity in the STIR image (B). A slight convexity of the posterior wall is shown in the CT scan (C). The bone marrow in other vertebrae appears normal (arrrowheads).

suppression of signal on the opposed-phase images (Lecouvet *et al*, 1999; Hanrahan *et al*, 2010; Martí-Bonmatí *et al*, 2015).

Our study considered the more recent guidelines for the diagnostic work-up of MM (Moreau *et al*, 2013; Rajkumar *et al*, 2014), which recommend the use of WBULDCT and

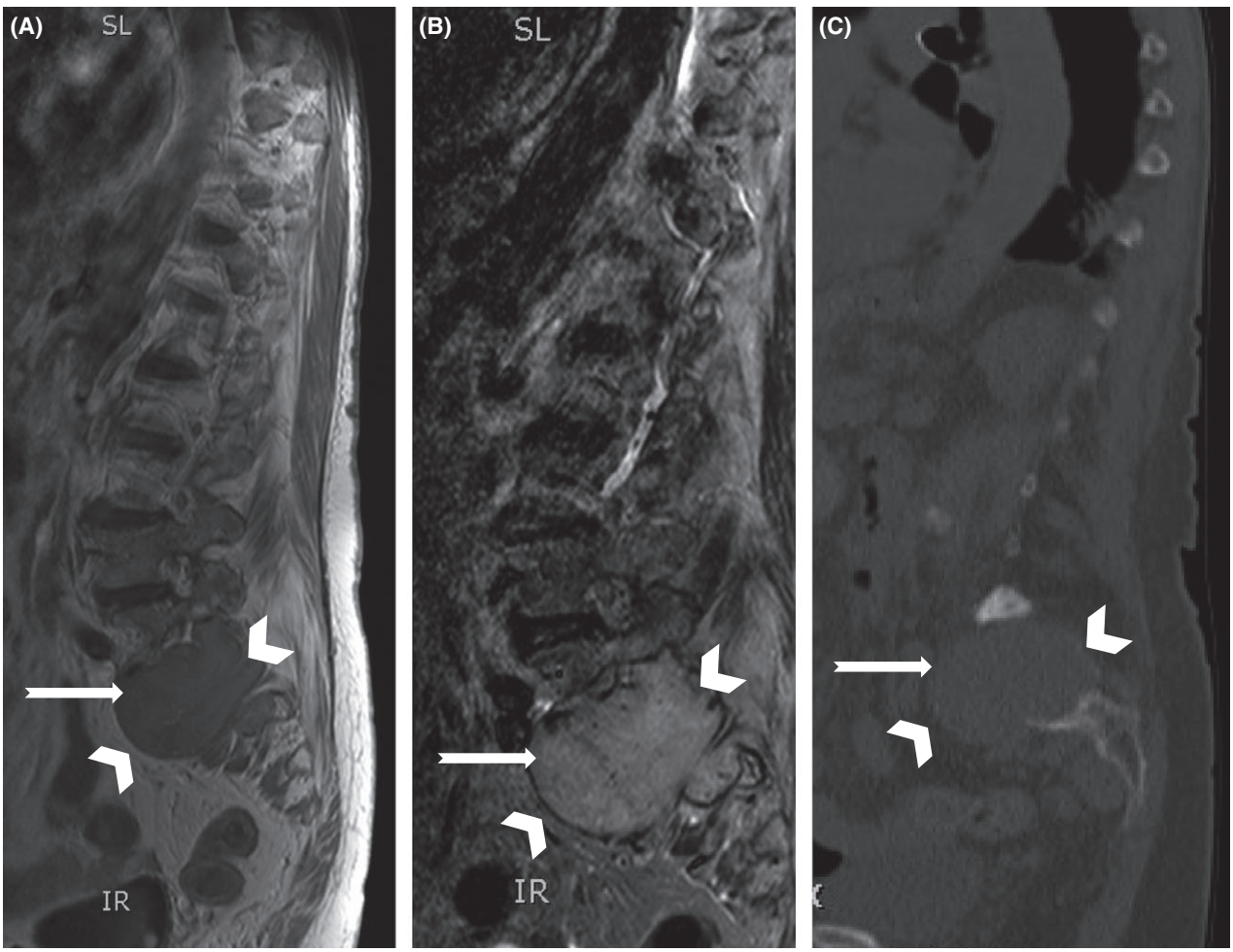

Fig 3. A 64-year-old patient with focal pattern evaluated during disease follow-up. Sagittal unenhanced T1-weighted (A), short tau inversion recovery (STIR) (B) and computed tomography (CT) scan image (C). Magnetic resonance images demonstrate a bulky mass involving the second sacral vertebra (arrrow) and extending into contiguous soft tissues with low signal intensity in T1 sequence (A), high signal intensity in STIR (B), and appearing in CT image (C) as a bulky osteolytic lesion with soft tissue density (arrow) with contiguos soft tissues involvement (arrowheads). This signal intensity pattern is characteristic of active multiple myeloma lesions.

MRI for the diagnosis and staging of the disease, by comparing the diagnostic value of WBULDCT with SMRI in the identification of spinal bone marrow involvement in MM patients.

WBULDCT and SMRI imaging were used to analyse the myelomatous spinal involvement in our series of 35 MM patients.

Bone marrow involvement was classified into 4 different patterns (focal, diffuse, combined and negative) according to the literature (Lecouvet *et al*, 1999; Hanrahan *et al*, 2010; Derlin & Bannas, 2014), and the infiltration patterns were concordant in both techniques, finding 11 focal patterns (31·42%), 5 diffuse patterns (14·28%), 11 combined patterns (31·42%) and 8 negative patterns (21·85%) (Table IV).

When analysing the spinal anatomic distribution of myelomatous lesions within the focal and combined pattern of disease, a preferred distribution within the dorsal spine on both techniques was found (Table V).

The overall concordance between WBULDCT and SMRI in the detection of myelomatous lesions within the axial skeleton was 76·7%. In particular, both techniques showed no evidence of myelomatous lesions in 8/35 (22·85%) patients, while they were both positive in 22/35 (62·85%).

WBULDCT and SMRI were discordant in only 2 (5·71%) patients: 1 patient was positive on WBULDCT and negative on SMRI and 1 patient was negative on WBULDCT and positive on SMRI (Table VI).

Considering the spinal anatomic distribution of the myelomatous lesions, the concordance was 61·6% on the cervical spine, 71·5% on the dorsal spine, 86·4% on the lumbar spine and 94·4% on the sacral spine, while the concordance according to the pattern of disease was 56·1% for the focal pattern and 88·7% for the combined pattern and the Cohen's kappa index demonstrated an excellent agreement in the assessment of disease (K = 0·85).

The agreement between WBULDCT and SMRI was also evaluated in terms of the Durie and Salmon Staging System Plus, which showed lower agreement (K = 0·66) when compared with that of the distribution pattern, but was statistically significant ($P < 0·005$) in the final assessment of disease (Table VII).

Our results highlight an excellent concordance between both techniques, suggesting their potential interchangeability in the evaluation of spinal myelomatous involvement (Fig 3).

These results may indicate the possibility of employing WBLDCT to evaluate the bone marrow of the entire skeleton in a single procedure, increasing the confidence of the reader in discriminating between senile osteoporosis and the diffuse bone pattern of MM: usually the bones of the head, upper arms and ribs are not commonly involved by benign osteoporosis, so if those bones present an osteoporotic pattern, especially at a relative young age (i.e. 40–60 years of age), the diagnosis of pathological diffuse bone involvement is more probable.

The present results are in agreement with those reported in literature; in particular the use of both WBULDCT and SMRI is recommended for the diagnostic workup of multiple myeloma by the most recent guidelines. The ESMO Guidelines Working Group (Moreau *et al*, 2013) and the IMWG (Rajkumar *et al*, 2014) acknowledged that CT and MRI are equally sensitive in the detection of MM bone lesions, recommending the use of these techniques to evaluate symptomatic bony sites, even if the skeletal survey is negative and the patient has symptoms suggesting bone lesions, and, in particular, stressing the importance of the MRI evaluation in cases of suspected spinal cord compression (Rajkumar *et al*, 2014; Martí-Bonmatí *et al*, 2015).

Conversely, Wight *et al* (2015) evaluated the detection rate of spinal myelomatous lesions in SMRI compared with Whole-Body MDCT in order to assess accuracy in staging. In their conclusions they asserted that screening by SMRI in asymptomatic patients had a low yield for focal spinal disease (recommending SMRI evaluation only in symptomatic patients) and that in patients with symptomatic myeloma requiring therapy with no clinical reason to evaluate the spine, SMRI evaluation is of questionable value as it adds little clinically useful information that will alter their management.

Some limitations in our study should be considered. Firstly, it is a retrospective study from a single institution. Moreover, the cohort of patients studied is small, thus not allowing evaluation of the significance of our data. And, finally, only one radiologist assessed the WBULDCT and SMRI images.

In conclusion, WBULDCT represents a useful diagnostic tool for the detection of spinal involvement in MM patients; also offering detailed information regarding extra-axial involvement, which could be potentially missed with dedicated SMRI examination. Considering its larger spread, lower cost and shorter time of acquisition, it is more readily available than SMRI.

SMRI might be reserved for symptomatic patients who have negative CT results, to clarify ambiguous CT findings or to better define the nature of vertebral collapses.

Disclosure

All the authors have no financial interest and no competing interest.

Authorship

Davide Ippolito, Sara Spiga and Valeria Besostri performed the research. Davide Ippolito, Fausto Rossini and Cammillo Talei Franzesi designed the study. Sara Pezzotta and Fausto Rossini contributed essential reagents or tools. Sara Spiga, Valeria Besostri and Sara Pezzotta analysed the data. Davide Ippolito, Fausto Rossini and Cammillo Talei Franzesi wrote the paper. Sandro Sironi and Fausto Rossini revised the paper.

References

Baur-Melnyk, A., Buhmann, S., Becker, C., Schoenberg, S.O., Lang, N., Bartl, R. & Reiser, M.F. (2008) Whole-body MRI versus whole-body MDCT for staging of multiple myeloma. *American Journal of Roentgenology*, **190**, 1097–1104.

Bird, J.M., Owen, R.G., D'Sa, S., Snowden, J.A., Pratt, G., Ashcroft, J., Yong, K., Cook, G., Feyler, S., Davies, F., Morgan, G., Cavenagh, J., Low, E. & Behrens, J.; Haemato-oncology Task-Force of British Committee for Standards in Haematology (BCSH) and UK Myeloma Forum. (2011) Guidelines for the diagnosis and management of multiple myeloma 2011. *British Journal of Haematology*, **154**, 32–75.

Collins, C.D. (2004) Multiple myeloma. *Cancer Imaging*, 14, 4 Spec No A:S47-53.

Derlin, T. & Bannas, P. (2014) Imaging of multiple myeloma: Current concepts. *World Journal of Orthopaedics*, **5**, 272–282.

Derlin, T., Peldschus, K., Münster, S., Bannas, P., Herrmann, J., Stübig, T., Habermann, C.R., Adam, G., Kröger, N. & Weber, C. (2013) Comparative diagnostic performance of ^{18}F-FDG PET/CT versus whole-body MRI for determination of remission status in multiple myeloma after stem cell transplantation. *European Radiology*, **23**, 570–578.

Dimopoulos, M., Terpos, E., Comenzo, R.L., Tosi, P., Beksac, M., Sezer, O., Siegel, D., Lokhorst, H., Kumar, S., Rajkumar, S.V., Niesvizky, R. & Moulopoulos, L.A.; Durie BG for the IMWG. (2009) International myeloma working group consensus statement and guidelines regarding the current role of imaging techniques in the diagnosis and monitoring of multiple Myeloma. *Leukemia*, **23**, 1545–1556.

Dimopoulos, M., Kyle, R., Fermand, J.P., Rajkumar, S.V., San Miguel, J., Chanan-Khan, A., Ludwig, H., Joshua, D., Mehta, J., Gertz, M., Avet-Loiseau, H., Beksaç, M., Anderson, K.C., Moreau, P., Singhal, S., Goldschmidt, H., Boccadoro, M., Kumar, S., Giralt, S., Munshi, N.C. & Jagannath, S.; International Myeloma Workshop Consensus Panel 3. (2011) Consensus recommendations for standard investigative workup: report of the International Myeloma Workshop Consensus Panel 3. *Blood*, **117**, 4701–4705.

Durie, B.G. & Salmon, S.E. (1975) A clinical staging system for multiple myeloma. Correlation of measured myeloma cell mass with presenting clinical features, response to treatment, and survival. *Cancer*, **36**, 842–854.

Durie, B.G., Kyle, R.A., Belch, A., Bensinger, W., Blade, J., Boccadoro, M., Child, J.A., Comenzo, R., Djulbegovic, B., Fantl, D., Gahrton, G., Harousseau, J.L., Hungria, V., Joshua, D., Ludwig, H., Mehta, J., Morales, A.R., Morgan, G., Nouel, A., Oken, M., Powles, R., Roodman, D., San Miguel, J., Shimizu, K., Singhal, S., Sirohi, B., Sonneveld, P., Tricot, G. & Van Ness, B.; Scientific Advisors of the International Myeloma Foundation. (2003) Myeloma management guidelines: a consensus report from the Scientific Advisors of the International Myeloma Foundation. *The Hematology Journal*, **4**, 379–398. Review. Erratum in: Hematol J. 2004;5:285.

Ghanem, N., Lohrmann, C., Engelhardt, M., Pache, G., Uhl, M., Saueressig, U., Kotter, E. & Langer, M. (2006) Whole-body MRI in the detection of bone marrow infiltration in patients with plasma cell neoplasms in comparison to the radiological skeletal survey. *European Radiology*, **16**, 1005–1014.

Gleeson, T.G., Moriarty, J., Shortt, C.P., Gleeson, J.P., Fitzpatrick, P., Byrne, B., McHugh, J., O'Connell, M., O'Gorman, P. & Eustace, S.J. (2009) Accuracy of whole-body low-dose multidetector CT (WBLDCT) versus skeletal survey in the detection of myelomatous lesions, and correlation of disease distribution with whole-body MRI (WBMRI). *Skeletal Radiology*, **38**, 225–236.

Hanrahan, C.J., Christensen, C.R. & Crim, J.R. (2010) Current concepts in the evaluation of multiple myeloma with MR imaging and FDG PET/CT. *Radiographics*, **30**, 127–142.

Horger, M., Kanz, L., Denecke, B., Vonthein, R., Pereira, P., Claussen, C.D. & Driessen, C. (2007) The benefit of using whole-body, low-dose, nonenhanced, multidetector computed tomography for follow-up and therapy response monitoring in patients with multiple myeloma. *Cancer*, **109**, 1617–1626.

Horger, M., Pereira, P., Claussen, C.D., Kanz, L., Vonthein, R., Denecke, B. & Driessen, C. (2008) Hyperattenuating bone marrow abnormalities in myeloma patients using whole-body non-enhanced low-dose MDCT: correlation with haematological parameters. *British Journal of Radiology*, **81**, 386–396.

Ippolito, D., Besostri, V., Bonaffini, P.A., Rossini, F., Di Lelio, A. & Sironi, S. (2013) Diagnostic value of whole-body low-dose computed tomography (WBLDCT) in bone lesions detection in patients with multiple myeloma (MM). *European Journal of Radiology*, **82**, 2322–2327.

Lecouvet, F.E., Malghem, J., Michaux, L., Maldague, B., Ferrant, A., Michaux, J.L. & Vande Berg, B.C. (1999) Skeletal survey in advanced multiple myeloma: radiographic versus MR imaging survey. *British Journal of Haematology*, **106**, 35–39.

Lecouvet, F.E., Dechambre, S., Malghem, J., Ferrant, A. & Vande Berg, B.C. (2001) Maldague baudouin bone marrow transplantation in patients with multiple myeloma: prognostic significance of MR imaging. *American Journal of Roentgenology*, **176**, 91–96.

Mahnken, A.H., Wildberger, J.E., Gehbauer, G., Schmitz-Rode, T., Blaum, M., Fabry, U. & Günther, R.W. (2002) Multidetector CT of the spine in multiple myeloma: comparison with MR imaging and radiography. *American Journal of Roentgenology*, **178**, 1429–1436.

Martí-Bonmatí, L., Ramirez-Fuentes, C., Alberich-Bayarri, Á. & Ruiz-Llorca, C. (2015) State-of-the-art of bone marrow imaging in multiple myeloma. *Current Opinion in Oncology*, **27**, 540–550.

Moreau, P., San Miguel, J., Ludwig, H., Schouten, H., Mohty, M., Dimopoulos, M. & Dreyling, M.; ESMO Guidelines Working Group. (2013) Multiple myeloma: ESMO clinical practice guidelines for diagnosis, treatment and follow-up. *Annals of Oncology*, **24** Suppl 6, vi133–137.

Moulopoulos, L.A., Dimopoulos, M.A. & Smith, T.L. (1995) Prognostic significance of magnetic resonance imaging in patients with asymptomatic multiple myeloma. *Journal of Clinical Oncology*, **13**, 251–256.

Pianko, M.J., Terpos, E., Roodman, G.D., Divgi, C.R., Zweegman, S., Hillengass, J. & Lentzsch, S. (2014) Whole-body low-dose computed tomography and advanced imaging techniques for multiple myeloma bone disease. *Clinical Cancer Research*, **20**, 5888–5897.

Rajkumar, S.V., Dimopoulos, M.A., Palumbo, A., Blade, J., Merlini, G., Mateos, M.V., Kumar, S., Hillengass, J., Kastritis, E., Richardson, P., Landgren, O., Paiva, B., Dispenzieri, A., Weiss, B., LeLeu, X., Zweegman, S., Lonial, S., Rosinol, L., Zamagni, E., Jagannath, S., Sezer, O., Kristinsson, S.Y., Caers, J., Usmani, S.Z., Lahuerta, J.J., Johnsen, H.E., Beksac, M., Cavo, M., Goldschmidt, H., Terpos, E., Kyle, R.A., Anderson, K.C., Durie, B.G. & Miguel, J.F. (2014) International Myeloma Working Group updated criteria for the diagnosis of multiple myeloma. *The Lancet. Oncology*, **15**, e538–e548.

Regelink, J.C., Minnema, M.C., Terpos, E., Kamphuis, M.H., Raijmakers, P.G., Pieters- van den Bos, I.C., Heggelman, B.G., Nievelstein, R.J., Otten, R.H., van Lammeren-Venema, D., Zijlstra, J.M., Arens, A.I., de Rooy, J.W., Hoekstra, O.S., Raymakers, R., Sonneveld, P., Ostelo, R.W. & Zweegman, S. (2013) Comparison of modern and conventional imaging techniques in establishing multiple myeloma-related bone disease: a systematic review. *British Journal of Haematology*, **162**, 50–61.

Sachpekidis, C., Mosebach, J., Freitag, M.T., Wilhelm, T., Mai, E.K., Goldschmidt, H., Haberkorn, U., Schlemmer, H.P., Delorme, S. & Dimitrakopoulou-Strauss, A. (2015) Application of (18)F-FDG PET and diffusion weighted imaging (DWI) in multiple myeloma: comparison of functional imaging modalities. *American Journal of Nuclear Medicine and Molecular Imaging*, **5**, 479–492.

Shortt, C.P., Breen, K.A., McHugh, J., O'Connell, M.J., O'Gorman, P.J. & Eustace, S.J. (2009) Whole-body MRI versus PET in assessment of multiple myeloma disease activity. *American Journal of Roentgenology*, **192**, 980–986.

Song, I.C., Kim, J.N., Choi, Y.S., Ryu, H., Lee, M.W., Lee, H.J., Yun, H.J., Kim, S., Kwon, S.T. & Jo, D.Y. (2015) Diagnostic and prognostic implications of spine magnetic resonance imaging at diagnosis in patients with multiple myeloma. *Cancer Research and Treatment*, **47**, 465–472.

Spinnato, P., Bazzocchi, A., Brioli, A., Nanni, C., Zamagni, E., Albisinni, U., Cavo, M., Fanti, S., Battista, G. & Salizzoni, E. (2012) Contrast enhanced MRI and ^{18}F-FDG PET-CT in the assessment of multiple myeloma: a comparison of results in different phases of the disease. *European Journal of Radiology*, **81**, 4013–4018.

Terpos, E., Kleber, M., Engelhardt, M., Zweegman, S., Gay, F., Kastritis, E., van de Donk, N.W., Bruno, B., Sezer, O., Broijl, A., Bringhen, S., Beksac, M., Larocca, A., Hajek, R., Musto, P., Johnsen, H.E., Morabito, F., Ludwig, H., Cavo, M., Einsele, H., Sonneveld, P. & Dimopoulos, M.A.; Palumbo A for the European Myeloma Network.. (2015) European Myeloma Network guidelines for the management of multiple myeloma-related complications. *Haematologica*, **100**, 1254–1266.

Weinstein, R.S. (1992) Bone involvement in multiple myeloma. *American Journal of Medicine*, **93**, 591–594.

Wight, J., Stillwell, A., Morris, E., Grant, B., Lai, H.C. & Irving, I. (2015) Screening whole spine magnetic resonance imaging in multiple myeloma. *Internal Medicine Journal*, **45**, 762–765.

Zamagni, E. & Cavo, M. (2012) The role of imaging techniques in the management of multiple myeloma. *British Journal of Haematology*, **159**, 499–513.

Zamagni, E., Patriarca, F., Nanni, C., Zannetti, B., Englaro, E., Pezzi, A., Tacchetti, P., Buttignol, S., Perrone, G., Brioli, A., Pantani, L., Terragna, C., Carobolante, F., Baccarani, M., Fanin, R., Fanti, S. & Cavo, M. (2011) Prognostic relevance of 18-F FDG PET/CT in newly diagnosed multiple myeloma patients treated with up-front autologous transplantation. *Blood*, **118**, 5989–5995.